



MINISTRY OF TECHNOLOGY

AERONAUTICAL RESEARCH COUNCIL

CURRENT PAPERS

LIBRARY
ROYAL AIRCRAFT ESTABLISHMENT
BEDFORD.

The Calculation of Momentum Thickness in a Turbulent Boundary Layer at Mach Numbers up to Unity

By

J. F. Nash and Miss A. G. J. Macdonald

LONDON: HER MAJESTY'S STATIONERY OFFICE

1967

Price 6s. 6d. net

July, 1966

The Calculation of Momentum Thickness in a Turbulent
Boundary Layer at Mach Numbers up to Unity

- By -

J. F. Nash and A. G. J. Macdonald

SUMMARY

For boundary layers of a class which includes those developing in "rooftop" pressure distributions, the small departures from local equilibrium (Nash¹) which occur are shown to have an even smaller effect on the growth of momentum thickness. The assumption of precise local equilibrium thus provides a simple but accurate basis for predictions of momentum thickness, and a calculation method is formulated accordingly.

List of Contents

	<u>Pages</u>
List of Symbols	2
1. Introduction	3
2. The Momentum Equation in Incompressible Flow	4
3. Comparison with Experiment and with other Methods	7
4. Compressibility Effects	8
5. Conclusions	9
Appendix I - Summary of Important Formulae	11
Appendix II - Algol Program of Calculation Method	13
References	22

List/

*Replaces NPL Aero Report 1207 - A.R.C.28 235.

List of Symbols

- x, y co-ordinates measured along and normal to the surface, respectively
- p static pressure
- u mean velocity in x-direction
- M Mach number
- ρ density
- ν kinematic viscosity
- T static temperature
- δ^* displacement thickness:-

$$\delta^* = \int_0^{\infty} \left(1 - \frac{\rho u}{\rho_e u_e} \right) dy$$

- θ momentum thickness:-

$$\theta = \int_0^{\infty} \frac{\rho u}{\rho_e u_e} \left(1 - \frac{u}{u_e} \right) dy$$

- H shape factor:- $H = \delta^*/\theta$

- G shape factor:-

$$G = \left(\frac{\rho_e}{\tau_w} \right)^{\frac{1}{2}} \cdot \frac{\int_0^{\infty} (u_e - u)^2 dy}{\int_0^{\infty} (u_e - u) dy}$$

- in incompressible flow:-

$$G = \left(\frac{\rho u_e^2}{\tau_w} \right)^{\frac{1}{2}} \left(1 - \frac{1}{H} \right)$$

- τ_w wall shear stress

- Π pressure-gradient parameter:-

$$\Pi = \frac{\delta^* dp}{\tau_w dx}$$

Subscripts

- e value at edge of boundary layer
w value at wall
 ∞ some reference value (free stream, e.g.)

Note

The symbol $f()$ denotes any arbitrary function.

1. Introduction

The prediction of the profile drag of two-dimensional aerofoils depends on the availability of an accurate method for calculating the growth of momentum thickness in the turbulent boundary layer at subsonic and transonic speeds.

The present work is mainly concerned with boundary layers developing in pressure distributions not too far from the "flat rooftop" type which consists of a run of constant pressure followed by a linear or near-linear pressure rise. This type of pressure distribution is obtained on many practical aerofoils at their design (cruise) condition. The maximum local Mach number is usually not much above unity (the "sonic rooftop" section is designed for $M \approx 1$ over the constant-pressure plateau). Over this restricted range of conditions there is good reason to expect simple boundary-layer techniques to apply. The treatment of boundary layers negotiating leading-edge suction peaks is considerably more difficult and will not be dealt with in detail in this paper.

The treatment of boundary layers in which the pressure-gradient parameter $\Pi \left(= \frac{\delta^*}{\tau_w} \frac{dp}{dx} \right)$ satisfies the condition $d\Pi/dx > 0$, which includes the case of the "rooftop" pressure distribution, is simple because the shape of the mean velocity profile is principally a function of the local pressure gradient¹, and only the thickness of the layer significantly reflects the influence of upstream history. To use the terminology of Ref. 1, the departures from local equilibrium are small. It will be shown in Section 2 that the effect of these departures from equilibrium on the growth of momentum thickness is even smaller. Indeed the assumption of precise local equilibrium is a valid approximation for many purposes. In the present paper this assumption is used as the basis of a calculation method which is more simple than the advanced methods currently being developed, but whose range of validity is limited to the types of pressure distribution under consideration.

In Section 3 comparisons are made with measurements in incompressible flow and with the predictions of other calculation methods. Section 4 consists of a discussion of the effects of compressibility on the momentum equation and on the local-equilibrium assumption.

In the present calculations use has been made of the skin-friction law specified in Ref. 2. This was based on the work of Nash³ and Spalding and Chi⁴. The relevant expressions are reproduced here in Appendix I.

The present method has already been used extensively for profile-drag predictions. A preliminary note¹⁷ has already been issued reporting some of this work.

2. The Momentum Equation in Incompressible Flow

2.1 The growth of a turbulent boundary layer in two dimensions is calculated by integrating the momentum-integral equation

$$\frac{d}{dx} (\rho_e u_e^2 \theta) = \tau_w (1 + \Pi), \quad \dots(1)$$

where

$$\Pi = \frac{\delta^* dp}{\tau_w dx}, \quad \dots(2)$$

along the surface, simultaneously with a skin-friction law (such as that described in Ref. 2) and an auxiliary equation. Equation (1) can also be written in the form:-

$$\frac{d\theta}{dx} = - (H + 2 - M_e^2) \frac{\theta}{u_e} \frac{du_e}{dx} + \frac{\tau_w}{\rho_e u_e^2}. \quad \dots(3)$$

Instead of specifying an auxiliary equation at the outset we shall examine the consequences of making various assumptions about the $G \sim \Pi$ trajectories of boundary layers of the type being considered. The subsequent discussion in this Section will be restricted to incompressible flow. Compressibility effects will be discussed in Section 4.

2.2 Equilibrium turbulent boundary layers are characterised by a particular, constant, value of the pressure-gradient parameter Π and a corresponding, constant, value of the shape factor G . All possible equilibrium boundary layers are represented by a unique function $G(\Pi)$. Fig. 1 shows this function for positive values of Π . An empirical fit to the experimental data is given by

$$G = 6.1 (\Pi + 1.81)^{\frac{1}{2}} - 1.7, \quad \dots(4)$$

as suggested in Ref. 1.

Boundary layers developing in arbitrary pressure gradients do not in general satisfy the condition $\Pi = \text{constant}$, and usually both Π and G are functions of x . If G is plotted against Π , for a particular boundary layer, a trajectory is obtained along which x varies. It is a property of a boundary layer for which Π increases monotonically with x that the trajectory lies close to the locus of all possible equilibrium boundary layers¹. Fig. 2 illustrates this behaviour with two sets of experimental data. This situation can be described as "local equilibrium" but the notion should not be misinterpreted. The correspondence to actual equilibrium boundary layers does not, for instance, extend to the shear stresses⁵ except at the wall.

2.3 If any relation is specified connecting G and Π , and use is made of a skin-friction law

$$\frac{\tau_w}{\rho_e u_e^2} = f \left(\frac{u_e \theta}{\nu}, G \text{ or } H \right), \quad \dots(5)$$

equation (1)/

equation (1) (or (3)) can be reduced to the form

$$\frac{d\theta}{dx} = f \left(\frac{u_e \theta}{\nu}, - \frac{\theta}{u_e} \frac{du_e}{dx} \right). \quad \dots(6)$$

The assumption of precise local equilibrium, which corresponds to an exact correlation between the $G \sim \Pi$ trajectory and the equilibrium locus (equation (4)), together with the skin-friction law of Ref. 2, leads to the function plotted in Fig. 3. The derivative $d\theta/dx$ is roughly a linear function of $-(\theta/u_e) du_e/dx$ and, over a limited range of Reynolds number, the effect of variations of $u_e\theta/\nu$ is approximately independent of the pressure gradient. The contribution of the skin-friction term to $d\theta/dx$ is small except for very small pressure gradients. Separation is predicted when $-(\theta/u_e) du_e/dx$ reaches a value of about 0.004; $d\theta/dx$ reaches a value of about 0.02 at separation, which agrees with the figure suggested by McQuaid⁶.

2.4 The effect on $d\theta/dx$ of departures from local equilibrium can be assessed by taking a relation between G and Π different from the equilibrium one. The boundary layers on rooftop aerofolds are usually in equilibrium at the start of the pressure rise (that is, at the end of the run of constant pressure) and the departures from local equilibrium occur for values of Π greater than zero. In Fig. 4 calculations are illustrated assuming that the values of $G - 6.5$ are 50 percent above and below the local equilibrium values. The results are also tabulated in Table 1. It is seen that these gross departures from equilibrium do not have a marked effect on $d\theta/dx$, particularly if the departures are in the direction of the curve "A" in Fig. 4 (inset).

Table 1

Values of $d\theta/dx$ for $u\theta/\nu = 10^4$ (see also Fig. 4)

$\frac{\theta}{u} \frac{du}{dx}$	local equilibrium $d\theta/dx$	$G - 6.5$ 50% high:-		$G - 6.5$ 50% low:-		"frozen"	
		$d\theta/dx$	% diff.	$d\theta/dx$	% diff.	$d\theta/dx$	% diff.
0×10^3	1.32×10^3	1.32	0	1.32	0	1.32	0
0.5	2.88	2.83	-1.7	2.93	+1.7	2.97	+3.1
1.0	4.51	4.46	-1.1	4.58	+1.6	4.63	+2.7
1.5	6.20	6.23	+0.5	6.23	+0.5	6.28	+1.3
2.0	8.03	8.67	+8.0	7.97	-0.7	7.94	-1.1
2.5	9.92			9.69	-2.3	9.59	-3.3
3.0	12.00			11.44	-4.7	11.25	-6.3

The limiting case of a trajectory lying below the equilibrium locus would be the case $G = \text{constant}$. This might correspond to a situation where the pressure gradient was applied so rapidly that the boundary layer did not have time to respond. H , and τ_w also if the skin-friction law continued to hold,

would/

would be "frozen" at their initial values at the start of the pressure rise. Even in such a case the effect on $d\theta/dx$ is not large (Table 1).

The insensitivity of $d\theta/dx$ to departures from local equilibrium can be explained by noting that $d\theta/dx$ is the sum of two terms (see equation (3)) which have a dependence on G of opposite sign. A decrease, say, of G leads to a decrease of the pressure-gradient term and to an increase of the skin-friction term, and vice versa. Departures from local equilibrium thus have an appreciable effect on the ratio of the two terms but little effect on their sum.

2.5 The conclusion from the work in Section 2.4 is that, for boundary layers in which $d\Pi/dx > 0$, it is not necessary to predict the departures from equilibrium in any detail for the purposes of calculating the rate of growth of momentum thickness. Indeed, in most cases, the assumption of precise local equilibrium would appear to be adequate. A calculation method based on this assumption is specified by equations (1) (or (3)) and (4), together with the definitions of the various quantities and a skin-friction law. All the necessary equations are listed again in Appendix I(a). Values of the other integral parameters are provided by the calculation method, although these will not generally be so accurate as the predicted values of θ . The analysis of experimental data in Ref. 1 suggested that the assumption of local equilibrium could give predictions of H which are accurate to about ± 10 percent for values of Π up to 12. The predicted values of Π can be examined to check that $d\Pi/dx > 0$ and hence that the method is being used within its range of validity.

If momentum thickness only is required, an approximation to the full equations can be obtained by fitting an empirical expression to the curves in Fig. 3. A possible form of such an expression is:-

$$\frac{d\theta}{dx} = \left\{ 2.4711 \ln \left(\frac{u_e \theta}{\nu} \right) + 4.75 \right\}^{-2} - 3 \frac{\theta}{u_e} \frac{du_e}{dx} + 120 \left(\frac{\theta}{u_e} \frac{du_e}{dx} \right)^2 - 25\,000 \left(\frac{\theta}{u_e} \frac{du_e}{dx} \right)^3 \quad \dots(7)$$

2.6 An expression for $d\theta/dx$ of the form of equation (6) is also a feature of the "quadrature" methods for calculating momentum thickness. A number of such methods can be found in the literature. Specifically, these methods assume a linear dependence of $d\theta/dx$ on $-(\theta/u_e) du_e/dx$ and a power law for skin friction:-

$$\frac{d\theta}{dx} = a \cdot \left(\frac{u_e \theta}{\nu} \right)^{-b} - c \cdot \frac{\theta}{u_e} \frac{du_e}{dx} \quad \dots(8)$$

The values of the constants a , b and c vary from one method to another; on page 81 of Ref. 7 seven sets of these constants are listed as suggested by different authors.

The quadrature methods imply the existence of some local-equilibrium condition* (not necessarily a physically realistic one), and Fig. 5 shows that they can be regarded as the results of attempts to approximate the correct variation of $d\theta/dx$ with $-(\theta/u_e) du_e/dx$ by a straight line. It is clear that this cannot be done with any accuracy over the full range of pressure gradients and the quadrature methods are thus of limited value. Buri's value of c is about the most realistic compromise.

3. Comparison with Experiment and with other Methods

The justification for the use of the local-equilibrium assumption, over its range of validity, as a basis for calculating momentum thickness has been argued from a theoretical standpoint in the previous Sections. Comparisons with experiment are therefore not essential. Nevertheless it will be reassuring to make one such comparison with a suitable set of measurements. Another comparison will be made with an experiment which did not conform to the restriction $d\Pi/dx > 0$. Here the method is being used outside its range of validity and the interest is merely in seeing what order of inaccuracy is introduced.

The first comparison is with the measurements by Schubauer and Spangenberg¹⁹ in their pressure distribution "D". This boundary layer exhibits a monotonic increase of Π with x and approximates to local-equilibrium growth (see Fig. 2). The results are shown in Fig. 6. The experiment was not exactly two-dimensional and the corresponding discrepancies in the momentum equation are indicated in the figure. Predictions** by the methods of Head²⁰, McDonald and Stoddart²¹ and Bradshaw et al²² are also shown in Fig. 9. All four sets of predictions are within the experimental accuracy. The difference between our value of θ at $x = 110$ inches and that given by Head's method is no more than can be accounted for by a 10 percent error in θ at $x = 0$. In this example the local-equilibrium method is in good agreement both with measurement and with more sophisticated calculation methods.

The second comparison is with measurements by Bradshaw and Ferriss¹⁸ in a boundary layer initially developing in an adverse pressure gradient which is subsequently removed. In this case $d\Pi/dx < 0$ and substantial departures from local equilibrium occur (see Ref. 1). The results in Fig. 7 show that $d\theta/dx$ is overestimated throughout. For $x > 60$ inches, the pressure gradient is effectively zero and the overestimate of $d\theta/dx$ can be accounted for simply in terms of the amount by which G exceeds its equilibrium value. For $\Pi = 0$, and $u_e \theta/\nu = 10^4$, the error in $d\theta/dx$ is as follows:-

G	Error, %
15	83
10	31
8	12
6.5	0

At/

* It is only the expressions for momentum thickness that imply the assumption of local equilibrium. It must be stressed that no such interpretation can be made of the auxiliary equations also derived by some of these authors, except in the case of Buri¹¹ who suggested the local equilibrium concept in 1931.

** The calculated results for the methods of Head, and McDonald and Stoddart were taken from Ref. 21. The authors are indebted to Mr. Bradshaw for supplying the results for the method of Ref. 22.

At $x = 95$ in. θ is overestimated by about 6 percent. If the run of constant pressure had extended indefinitely, the error in θ would probably not have increased indefinitely since the error in $d\theta/dx$ would have decreased to zero as G approached its equilibrium value.

The other calculation methods give more accurate predictions of θ , in Fig. 7, according to the extent to which they take account of the physical processes involved. As noted in Ref. 18 this is a good boundary layer for exposing weaknesses in prediction methods.

4. Compressibility Effects

The extension of the local-equilibrium method to compressible flow depends on the availability of a suitable skin-friction law (which has been discussed in Ref. 2) and of some expression for the locus of all possible equilibrium boundary layers at non-zero Mach number. The momentum-integral equation remains unchanged (equation (1)).

In any discussion of equilibrium boundary layers in compressible flow speculation plays the major role because no relevant data exist. However in the present context the lack of definitive information is not a major obstacle. The two main reasons for this are:-

- (a) The Mach-number range under consideration ($0 < M_e < 1$) is not large, so that the effects of compressibility are unlikely to be dominant.
- (b) A corollary of the fact that $d\theta/dx$ is largely insensitive to departures from equilibrium (which carries over to compressible flow much as described in Section 2.4) is the fact that the $G \sim \Pi$ locus for equilibrium boundary layers does not have to be specified very accurately for the purpose of predicting accurate values of θ under local-equilibrium conditions.

In view of these two observations we feel justified in assuming that equation (4) is valid for our calculations in compressible flow. The definition of Π remains the same as in incompressible flow and G is defined, and related to the other integral parameters, as described in Ref. 2, i.e.,

$$G = \left(\frac{\rho_e}{\tau_w} \right)^{\frac{1}{2}} \frac{\int_0^{\infty} (u_e - u)^2 dy}{\int_0^{\infty} (u_e - u) dy}, \quad \dots(9)$$

$$= \left(\frac{\rho_e u_e^2}{\tau_w} \right)^{\frac{1}{2}} \left(1 - \frac{1}{\bar{H}} \right), \quad \dots(10)$$

where
$$\bar{H} = \frac{H + 1}{1 + 0.178 M_e^2} - 1. \quad \dots(11)$$

On this basis the relation between $d\theta/dx$ and $-(\theta/u_e) du_e/dx$ can be calculated and is illustrated in Fig. 8 as a function of Mach number. The general trend is a decrease of $d\theta/dx$ with increasing Mach number over most of the range of pressure gradients. To provide a comparison with these calculations the results are also shown of applying the Stewartson/Mager transformation²⁴ to the results for $M_e = 0$. The values of $d\theta/dx$ obtained by the two methods are approximately the same for small pressure gradients but the Mager transformation predicts a much more rapid decrease (with increasing Mach number) of $-(\theta/u_e) du_e/dx$ at separation and would thus predict an earlier separation in the same velocity distribution. This tendency would be aggravated by the higher values of $d\theta/dx$ predicted by the Mager transformation for large pressure gradients.

To illustrate the predicted effect of Mach number on the growth of momentum thickness, calculations have been made, using the present method, on the same velocity distribution, u_e/u_∞ , as considered in Fig. 6, with the same origin of the boundary layer and Reynolds number, but for $M_\infty = 1$. These results are shown in Fig. 9. Calculations were also made using the alternative form of the skin-friction law proposed in Ref. 2 (i.e., equation (9) of Ref. 2); the predicted values of θ were indistinguishable from the former calculations.

Consistent with Fig. 8, the growth of momentum thickness is less in compressible than in incompressible flow. At $x = 120$ inches the value of θ is about 24 percent lower than for $M_\infty = 0$; of this 24 percent, about 6 percent is the result of the difference in θ at $x = 0$. As a comparison with the calculations using the present method, Fig. 9 also shows the predictions by the quadrature method of Spence²⁵ which involves a transformation based on Eckert's intermediate-enthalpy method for flat-plate skin friction. At both $M_\infty = 0$ and 1 the predictions using the method of Spence lie above the present predictions (see Section 2.6 and Fig. 5). The decrement in θ due to compressibility is, however, of roughly the same order as indicated by the present calculations. This (to borrow a phrase from Dr. Spence's paper) is reassuring but does not necessarily mean the answers are correct.

5. Conclusions

1. For turbulent boundary layers in which the pressure-gradient parameter $\Pi \left(= \frac{\delta^*}{\tau_w} \frac{dp}{dx} \right)$ increases monotonically with x (a class which includes those developing in "rooftop" pressure distributions), such departures from local equilibrium that occur at all (see Nash¹) have a small effect on the growth of momentum thickness. Accurate predictions of momentum thickness in incompressible flow can be made on the assumption of precise local equilibrium. On this basis the usual "auxiliary equation" appearing in the calculation methods can be replaced by a simple algebraic relation which expresses the locus of all possible equilibrium boundary layers in the shape-factor/pressure-gradient plane. The values of the other integral parameters are obtained from the calculation method but these must be regarded as less reliable than the predicted momentum thicknesses. It can be checked that the method is being used within its range of validity by examining the predicted variation of Π with x .

2. The extension of the local-equilibrium concept to compressible flow depends only on the specification of the appropriate equilibrium loci. Even though no relevant experimental data exist as to their position, a provisional assumption is regarded as sufficiently accurate for the purposes of calculating momentum thickness for Mach numbers up to one.

3. The calculation method for subsonic and transonic speeds is specified by the equations listed in Appendix I. An Algol computer program using the method for calculating the boundary-layer development over two-dimensional aerofoils is shown in Appendix II.

APPENDIX I/

APPENDIX I

Summary of Important Formulae

A. Full Equations

1. Momentum equation:-

$$\frac{d}{dx} (\rho_e u_e^2 \theta) = \tau_w (1 + \Pi),$$

or
$$\frac{d\theta}{dx} = - (H + 2 - M_e^2) \frac{\theta}{u_e} \frac{du_e}{dx} + \frac{\tau_w}{\rho_e u_e^2}.$$

2. Skin-friction law (Ref. 2):-

$$\frac{\tau_w}{\rho_e u_e^2} = \left[F_c^{\frac{1}{2}} \cdot \left\{ 2.4711 \ln \left(F_R \cdot \frac{u_e \theta}{\nu_e} \right) + 4.75 \right\} + 1.5G + \frac{1724}{G^2 + 200} - 16.87 \right]^{-2},$$

with
$$F_c^{\frac{1}{2}} = 1 + 0.066 M_e^2 - 0.008 M_e^3,$$

$$F_R = 1 - 0.134 M_e^2 + 0.027 M_e^3.$$

3. "Auxiliary equation" (equilibrium locus):-

$$G = 6.1 (\Pi + 1.81)^{\frac{1}{2}} - 1.7.$$

4. Relation between G, H and τ_w :-

$$H = (\bar{H} + 1)(1 + 0.178 M_e^2) - 1,$$

with
$$\bar{H} = \left\{ 1 - G \left(\frac{\tau_w}{\rho_e u_e^2} \right)^{\frac{1}{2}} \right\}^{-1}.$$

5. Definition of Π :-

$$\Pi = \frac{\delta^* dp}{\tau_w dx} = - \frac{H}{\left(\frac{\tau_w}{\rho_e u_e^2} \right)} \cdot \frac{\theta}{u_e} \frac{du_e}{dx}$$

B. Approximation for Incompressible Flow

For $10^3 < \frac{u_e \theta}{\nu} < 10^5$ an approximation to equations (1) to (5) above is given by

$$\begin{aligned} \frac{d\theta}{dx} = & \left\{ 2.4711 \ln \left(\frac{u_e \theta}{\nu} \right) + 4.75 \right\}^{-2} \\ & - 3 \frac{\theta}{u_e} \frac{du_e}{dx} + 120 \left(\frac{\theta}{u_e} \frac{du_e}{dx} \right)^2 \\ & - 25\,000 \left(\frac{\theta}{u_e} \frac{du_e}{dx} \right)^3. \end{aligned}$$

APPENDIX II

ALGOL Program

A specimen Algol program using the local-equilibrium calculation method is shown below together with the relevant input instructions. At the N.P.L. the program is run on an English Electric-Leo-Marconi KDF9 machine. The running time is less than 2 minutes per run.

The program is for the calculation of the boundary-layer growth over a thick aerofoil specified by rectangular co-ordinates X, Y , (arbitrarily spaced chordwise stations). The pressure distribution can be specified in terms of u_e/u_∞ , C_p or p/p_{total} . An interpolation is made to find the pressures/velocities at evenly spaced points along the surface of the aerofoil. The isentropic-flow relations are used to derive arrays of u_e/u_∞ and T_e/T_∞ for use in the subsequent calculations.

Up to three chord Reynolds numbers and three transition positions can be specified per run. The laminar boundary layer is calculated using Thwaites method²⁶, together with the Stewartson transformation. Continuity of momentum thickness is assumed at the transition point so long as $u_e \theta / \nu_e > 320$; if it does not θ is increased to make $u_e \theta / \nu_e = 320$, (see Refs. 17, 27).

The turbulent boundary-layer equations (see Appendix I, above) are solved by a step-by-step process. An iteration is performed, involving θ , Π , G , τ_w and H , over two forward points. When the process has converged the integral parameters are known more accurately at the first forward point than at the second. The calculation then moves forward one step; the values are already known approximately at the new first forward point and can be improved by the subsequent iteration. Approximate values are also derived at the new second forward point, and so on. Integrations are performed by fitting quadratic expressions to the integrands over the three points and then integrating the quadratics.

This procedure is fast and has the advantage that relatively few steps are required for most purposes. The calculation shown in Fig. 6 was performed using intervals in x of 4 inches and 10 inches. The predicted values of θ at $x = 110$ inches agreed to within 0.25 percent.

The output from the program consists of tabulated values of θ , δ^* , Π , G , H and τ_w . The values of θ are, of course, relatively insensitive to departures from local equilibrium whereas the same is not true of the other integral parameters, and the predicted values of these should be treated with caution.

Calculation method based on local equilibrium

ALGOL PROGRAM

```

begin library AO,A6;
  real m1,ds,dsr;
  integer ic,nc,i,i1,dir,l,f,ff,fs,fc;
  array u[0:100],t[0:100],xt[1:3],re[1:3];

  procedure int(x1,y1,x2,y2,x3,y3,a,b,c,fail);
  value x1,y1,x2,y2,x3,y3;
  real x1,y1,x2,y2,x3,y3,a,b,c;
  label fail;
  begin real d;
    d=(x3-x2)*(x2-x1)*(x3-x1);
    if d=0 then goto fail;
    a:=(y1*(x2*x32-x22*x3)-y2*(x1*x32-x12*x3)+y3*(x1*x22-x12*x2))/d;
    b:=(-y1*(x32-x22)+y2*(x32-x12)-y3*(x22-x12))/d;
    c:=(y1*(x3-x2)-y2*(x3-x1)+y3*(x2-x1))/d;
  end,

  f:=format([6sd ddddd]);
  ff:=format([d. ddddd]);
  fs:=format([5s+d ddddd]);
  fc:=format([6sd dddddc]);
  open(20);
  open(30);
  nc:=read(20);
  for ic:=1 step 1 until nc do
  begin
  m1:=read(20);
  dir =read(20);
  l:=read(20);
  ds:=read(20);
  for i:=1 step 1 until 3 do
  re[i]:=read(20);
  for i =1 step 1 until 3 do
  xt[i]:=read(20);
  write text(30,[6s]Program*AP4[cc]);
  write text(30,[6s]M*=);
  write(30,format([sd. ddddc]),m1);
  end;
end;

```



```

begin comment Interpolation etc of input data;
real s, si, ss, sm, output, m, mb, angle, angle1, a, b, c;
integer j, h;
array x[1:3], y[1:3], input[1:3];
boolean cpi, phi;
write text(30, [[6s]s[12s]x[12s]y[12s]u/uinf[7s]t/tinf[7s]m[2c]]);
cpi := (dir=1);
phi := (dir=2);
ii := -1;
dsr := ds;
si = 0;
for j = 1 step 1 until 1 do
begin for h := 1, 2 do
begin x[h] := x[h+1];
y[h] := y[h+1];
input[h] := input[h+1];
end;
end;
x[3] := read(20);
y[3] := read(20);
input[3] := read(20);
if j < 3 then goto out;
s := sqrt((x[2]-x[1])2+(y[2]-y[1])2);
ss := sqrt((x[3]-x[2])2+(y[3]-y[2])2);
sm := (if j < 1 then s else s+ss+ds);
angle = if x[2]=x[1] then 1.5706 else arctan((y[2]-y[1])/(x[2]-x[1]));
if j=1 then angle1 := arctan((y[3]-y[2])/(x[3]-x[2]));
int(0, input[1], s, input[2], s+ss, input[3], a, b, c, fail);
for i := ii+1 step 1 until 100 do
begin si = (1-ii)*ds-dsr;
if si > sm then goto next;
output = a+b*si+c*si2;
if mi < 0.05 then goto incomp;
if phi then goto poh;
if not cpi then goto vel;
cp output = (1+0.7*mi2*output)/(1+0.2*mi2)3 5;
poh m = sqrt(5*(1/output10 2357143-1));
t[i] = (1+0.2*mi2)/(1+0.2*mi2);
u[i] = m/mixsqrt(t[i]);
goto print;
vel u[i] = output;

```

```

m:=mixu[1];
mb.=2;
for h:=1 step 1 until 10 do
begin
  m =u[1]xm1xqrt((1+0.2xm1t2)/(1+0.2xm1t2));
  if mb<10-4 then
  begin
    m =0;
    t[1].:=1+0.2xm1t2;
    goto print;
  end;
  if abs(1-m/mb)<10-3 then
  begin
    t[1].:=(1+0.2xm1t2)/(1+0.2xm1t2);
    goto print;
  end;
  mb'=m,
end;
incomp: if cpi then output =sqrt(abs(1-output));
u[1]:=output;
t[1]:=1;
print. write(30,f,1xds),
write(30,f,(if si<s then x[1]+s1xcos(angle) else x[2]+(si-s)xcos(angle1)));
write(30,fs,(if si<s then y[1]+s1xsin(angle) else y[2]+(si-s)xsin(angle1)));
write(30,f,u[1]);
write(30,f,t[1]);
write(30,fc,mixu[1]/sqrt(t[1]));
end;
next: i1=i-1;
dsr:=sm-s1+ds;
out
end;
write text(30,[[2c][6s]st*=[2c]]);
for h.=1,2,3 do
if xt[h]>0 then write(30,fc,xt[h]);
write text(30,[[2c][6s]trailing*edge.[2c]]);
write text(30,[[6s]s*=[6s]]);
write(30,ff,(i1-1)xds+dsr);
write text(30,[[c][6s]u/uinf*=[*]]);
write(30,ff,(u[i1-1]x(ds-dsr)+u[i1]xdsr)/ds);
write text(30,[[c][6s]t/tinf*=[*]]);
write(30,ff,(t[i1-1]x(ds-dsr)+t[i1]xdsr)/ds);
write text(30,[[p]]);
goto fin;
fail
fin.
end;
write text(30,[suspect*data]),
end;

```

```

begin comment Boundary layer calculation;
real integ,du,lambada,hh,li;
integer jr,jt,ft,ftc;
array theta[-1:100];
ft:=format([6sd,ddd,nd]);
ftc:=format([6sd,ddd,ndc]);
for jr:=1 step 1 until 3 do
begin if re[jr]<10 then goto outF;
write text(30,[[6s]laminar*boundary*layer[2c]]);
write text(30,[[6s]Re*=]);
write(30,format([sd,ddd,ndccc]),re[jr]);
write text(30,[[6s]s[12s]theta[10s]re(theta)[6s]delta[10s]h[12s]cf[2c]]);
integ:=0;
for i:=1 step 1 until li-1 do
begin integ:=integ+(5xu[1-1]1.5xt[1-1]1.5+8xu[1]1.5xt[1]1.5-u[1+1]1.5xt[1+1]1.5)
x0.08333333xds;
if integ<x-8 then integ:=x-8;
theta[1].:=0.667/u[1]1.5xsqrt(integ/re[jr]/t[1]1.5);
du:=-0.5x(u[1+1]-u[1-1])/ds;
lambada:=duxtheta[1]1.5xre[jr]x(1+0.2xmi1.2)xsqrt(t[1]);
if lambada>0.09 then lambada:=0.09;
if lambada>0 then
begin hh:=2+0.61xexp(6.283xlambada+495xlambada1.3);
li:=sqrt(0.0729-0.773xlambada)-0.05;
if lambada>0.089 then li:=0;
end else
begin hh:=2+0.983x(lambada+0.25)+5.83x(lambada+0.25)1.2;
li:=sqrt(0.0484-0.818xlambada);
end;
hh:=(hh+1)x(1+0.2xmi1.2)/t[1]-1;
write(30,f,ixds);
write(30,ft,theta[1]);
write(30,ft,theta[1]xu[1]xre[jr]xt[1]1.5);
write(30,ft,theta[1]xhh);
write(30,f,hh);
write(30,ftc,2xli/theta[1]xu[1]xt[1]/re[jr]);
end;
write text(30,[[p]]);

```

```

begin comment Turbulent boundary layer;
real gb,m,ren;
integer k,kk,fts,it,
array dlu,g,h,w,pi,integ[-1:1];
fts =format(['5s+d.ddd'+nd]);
for jt =1,2,3 do
begin if xt[jt]<0 then goto outt,
it =entier(xt[jt]/ds+0.5);
write text(30,['6s]turbulent*boundary*layer[2]);
write text(30,['6s]re*=]);
write(30,format(['d ddd'+ndccc]),re[jr]);
write text(30,['6s]s[12s]theta[10s]delta[10s]pi[13s]g[14s]h[12s]cf[2c]);
theta[0]:=0;
theta[1]:=theta[it];
if theta[1]xu[it]xt[it]^1.5xre[jr]<320 then
theta[1].:=320/(u[it]+v-6)/t[it]^1.5/re[jr];
dlu[1].:=u[it+1]/(u[it]+v-6)-1/ds;
g[1]:=6.5;
for kk:=1 step 1 until 10 do
begin m.=m1xu[it]/sqrt(t[it]);
ren.=re[jr]xtheta[1]xu[it]xt[it]^1.5x(1-0.134xm^2+0.027xm^3);
w[1].:=v+0.066xm^2-0.008xm^3)x(2.4711xln(ren+10)+4.75)+1.5xg[1]^1.724/
(g[1]^2+200)-16.87;
h[1].:=1/(1-g[1]/w[1]);
h[1].:=h[1]+1)x(1+0.178xm^2)/t[it]-1;
pi[1].:=theta[1]xh[1]xw[1]^2xdlu[1];
if pi[1]<-1.5 then pi[1].=-1.5;
g[1].:=6.1xsqrt(pi[1]+1.81)-1.7;
end;
integ[1].:=u[it]^2x(1+pi[1])xds/w[1]^2/3;
for i.=it step 1 until i1-1 do
begin for k.=1,0 do
begin dlu[k].:=dlu[k+1];
integ[k].:=integ[k+1];
theta[k].:=theta[k+1];
w[k].:=w[k+1];
pi[k].:=pi[k+1];
h[k].:=h[k+1];
g[k].:=g[k+1];
end;
end;

```

```

dlu[1] =if i<i1-1 then 0 5x(u[i+2]-u[i])/(u[i+1]+p-6)/ds else(1-u[i]/(u[i+1]+p-6))/ds;
if i=1 then goto cont;
pi[1] =2xpi[0]-pi[-1];
w[1] =2xw[0]-w[-1];
if pi[1]<-1 5 then pi[1] =-1 5;
if w[1]<10 then w[1] =10;
for kk.=1 step 1 until 10 do
begin
for k=0,1 do
integ[k] =u[i+k]t2xt[i+k]t2 5x(1+pi[k])xds/w[k]t2/3;
theta[0] =(u[i-1]t2xt[i-1]t2 5xtheta[-1]+1 25xinteg[-1]+2xinteg[0]-0 25xinteg[1])/
(u[i]t2+p-6)/t[i]t2 5;
theta[1] =(u[i-1]t2xt[i-1]t2 5xtheta[-1]+integ[-1]+4xinteg[0]+integ[1])/
(u[i+1]t2+p-6)/t[i+1]t2 5;
for k =0,1 do
begin
g[k] =6 1xsqrt(pi[k]+1 81)-1 7;
m.=m1xu[i+k]/sqrt(t[i+k]);
ren =re[jr]xtheta[k]xu[i+k]xt[i+k]t1 5x(1-0 134xm1t2+0 027xm1t3);
w[k] =(1+0.066xm1t2-0 008xm1t3)x(2 4711xln(ren+10)+4 75)+1 5xg[k]+1724/
(g[k]t2+200)-16 87;
h[k] =1/(1-g[k]/w[k]);
h[k] =(h[k]+1)x(1+0 173xm1t2)/t[i+k]-1;
pi[k] =-theta[k]xh[k]xw[k]t2xdlu[k];
if pi[k]<-1 5 then pi[k] =-1 5;
if pi[k]>w4 then pi[k] =w4;
if kk>5 and abs(1-gb/g[1])<0.005 then goto conv;
gb =g[1];
end;
end;
conv.
cont:
k=0;
write(30,f,(i+k)xds);
write(3,ft,theta[k]);
write(30,ft,theta[k]xh[k] ),
write(3,fts,pi[k]);
write(30,ft,g[k]);
write(3,f,h[k]);
if g[k]>600 then write(30,ftc,'') else
write(30,ftc,27/w[k]t2xu[i+k]t2xt[i+k]t2 5);

```

```

        if i=ii-1 and k=0 then
        begin    k:=1;
                goto cont;
        end;
    end;
    write text(30,[[2c][6s]trailing*edge:[2c]]);
    write text(30,[[6s]theta*=*]);
    write(30,ff,(theta[0]×(ds-dsr)+theta[1]×dsr)/ds);
    write text(30,[[c][6s]h*=[5s]]);
    write(30,ff,(h[0]×(ds-dsr)+h[1]×dsr)/ds);
    write text(30,[[p]]);
    outt:
    end;
    end;
    end;
    outr:  write text(30,[[p]]);

    close(20);
    close(30);

    end
    →

```

ALGOL PROGRAM

Specimen input

```

1;          ---number of cases
0.65;      ---Mach number
1;         ---program directive (0 for velocity, 1 for Cp, 2 for P/Ptotal)
15;        ---number of input values
0.05;      ---spacing of output points
n6; n7; n8; ---Reynolds numbers (put 0 if not required)
0.05; 0.2; 0.4; ---transition positions

```

<u>X/c</u>	<u>Y/c</u>	<u>input</u>
0;	0;	1.11000;
0.00961;	0.01329;	-1.06950;
0.03806;	0.02864;	-1.06950;
0.08427;	0.04440;	-1.06950;
0.14645;	0.05916;	-1.06950;
0.22221;	0.07143;	-1.06950;
0.30866;	0.08009;	-1.06950;
0.40245;	0.08315;	-1.03950;
0.50000;	0.07886;	-0.86247;
0.59755;	0.06874;	-0.66053;
0.69134;	0.05527;	-0.46634;
0.77779;	0.04043;	-0.28738;
0.85355;	0.02648;	-0.13052;
0.91573;	0.01494;	-0.00179;
1.0;	0;	0.17268;

```

→          ---end message

```

References

<u>No.</u>	<u>Author(s)</u>	<u>Title, etc.</u>
1	J. F. Nash	Turbulent-boundary-layer behaviour and the auxiliary equation. AGARDograph 97. A.R.C. C.P. 835, February, 1965.
2	J. F. Nash and A. G. J. Macdonald	A turbulent skin-friction law for use at subsonic and transonic speeds. A.R.C. C.P. 948, July, 1966.
3	J. F. Nash	A note on skin-friction laws for the incompressible turbulent boundary layer. A.R.C. C.P.862, December, 1964.
4	D. B. Spalding and S. W. Chi	The drag of a compressible turbulent boundary layer on a smooth flat plate with and without heat transfer. J. Fluid Mech., Vol.18, pp.117 - 143. 1964.
5	J. A. P. Stoddart	Some analysis of the constant velocity defect turbulent boundary layer. B.A.C. (Preston Division), Report Ae.260. May, 1966.
6	J. McQuaid	A velocity defect relationship for the outer part of equilibrium and near-equilibrium turbulent boundary layers. Communicated by Dr. L. C. Squire. A.R.C. C.P.885. October, 1965.
7	B. Thwaites (Ed.)	Incompressible Aerodynamics. Clarendon Press, Oxford. 1960.
8	E. Truckenbrodt	Ein Quadraturverfahren zur Berechnung der laminaren und turbulenten Reibungsschicht bei ebener und rotationssymmetrischer Strömung. Ing.-Arch., Vol. 20, pp.211 - 228. 1952.
9	D. A. Spence	The development of turbulent boundary layers. J. Aero. Sci., Vol.23, pp.3 - 15. 1956.
10	E. C. Maskell	Approximate calculation of the turbulent boundary layer in two-dimensional incompressible flow. R.A.E. Report No. Aero.2443. A.R.C.14. 654. November, 1951.

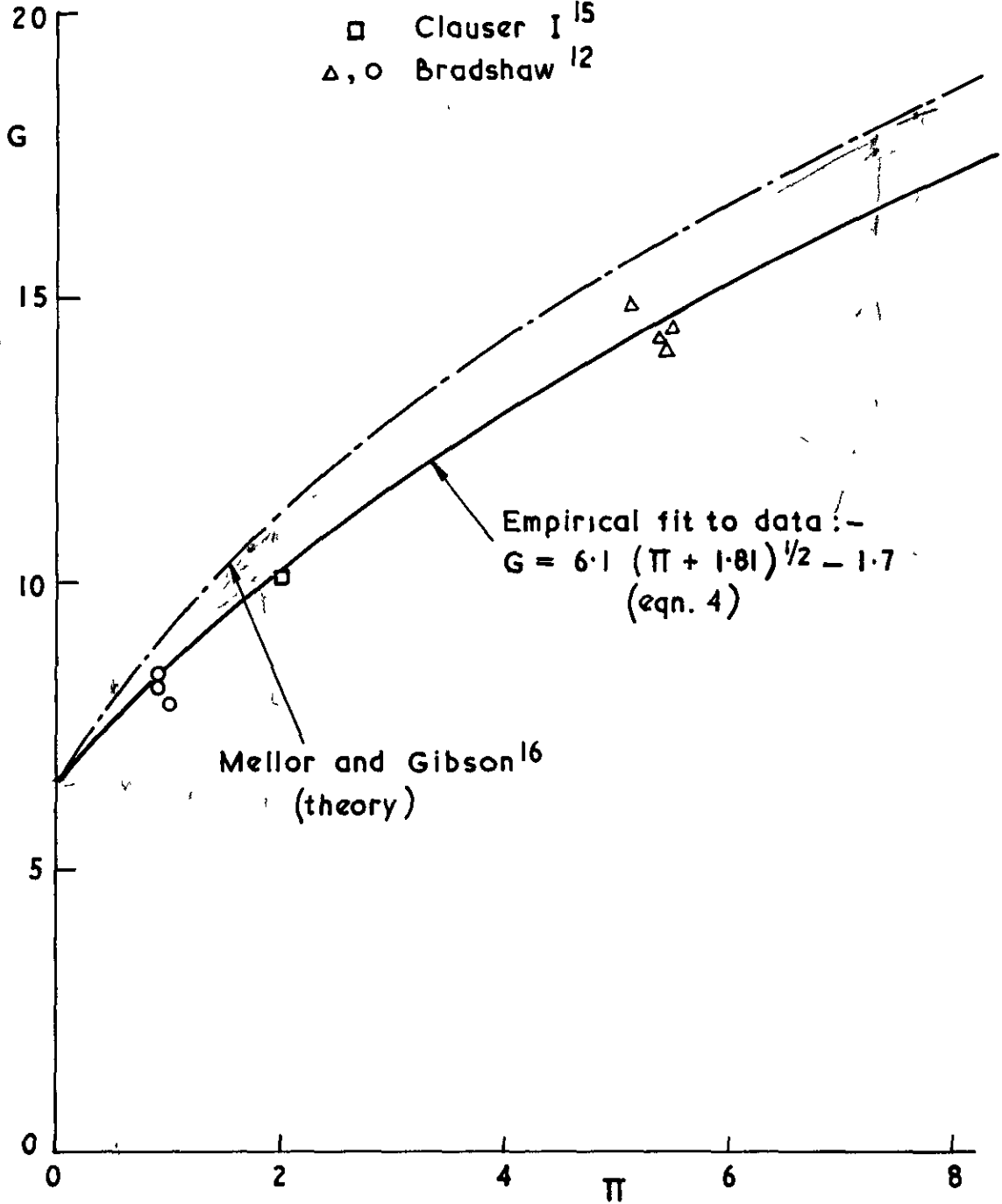
<u>No.</u>	<u>Author(s)</u>	<u>Title, etc.</u>
11	A. Buri	Eine Berechnungsgrundlage für die turbulente Grenzschicht bei beschleunigter und verzögerter Grundströmung. Diss. eidgen. tech. Hochsch., Zurich 652, 1931. (Translated as RTP Translation 2073)
12	P. Bradshaw	The turbulence structure of equilibrium boundary layers. NPL Aero Report 1184. A.R.C.27 675. January, 1966.
13	B. G. Newman	Some contributions to the study of the turbulent boundary-layer near separation. Dept. of Supply (Australia) Rep.ACA-53. March, 1951.
14	G. B. Schubauer and P. S. Klebanoff	Investigation of separation of the turbulent boundary layer. NACA Report 1030. 1951.
15	F. H. Clauser	The turbulent boundary layer. "Advances in Applied Mechanics", Vol.4. Academic Press. 1956.
16	G. L. Mellor and D. M. Gibson	Equilibrium turbulent boundary layers. J. Fluid Mech., Vol.24, pp.225 - 253 February, 1966.
17	J. F. Nash, J. Osborne and A. G. J. Macdonald	A note on the prediction of aerofoil profile drag at subsonic speeds. NPL Aero Report 1196. A.R.C.28 075. June, 1966.
18	P. Bradshaw and D. H. Ferriss	The response of a retarded equilibrium turbulent boundary layer to the sudden removal of pressure gradient. NPL Aero Report 1145. A.R.C.26 758. March, 1965.
19	G. B. Schubauer and W. G. Spangenberg	Forced mixing in boundary layers. J. Fluid Mech., Vol.8, Part 1, p.10 - 32. May, 1960.
20	M. R. Head	Entrainment in the turbulent boundary layer. A.R.C. R. & M.3152. September, 1958.
21	H. McDonald and J. A. P. Stoddart	On the development of the incompressible turbulent boundary layer. A.R.C. R. & M.3484. March, 1965.

<u>No.</u>	<u>Author(s)</u>	<u>Title, etc.</u>
22	P. Bradshaw, D. H. Ferriss and N. P. Atwell	Calculation of boundary-layer development using the turbulent energy equation. NPL Aero Report 1182. A.R.C.27 667. January, 1966.
23	D. Coles	The law of the wake in the turbulent boundary layer. J. Fluid Mech., Vol.1, Part 2, p.191. July, 1956.
24	A. Mager	Transformation of the compressible turbulent boundary layer. J. Ae. Sc., Vol.25, p.305. May, 1958.
25	D. A. Spence	The growth of compressible turbulent boundary layers on isothermal and adiabatic walls. A.R.C. R.&M.3191. June, 1959.
26	B. Thwaites	Approximate calculation of the laminar boundary layer. Aero Quart., Vol.1, p.245. 1949.
27	J. H. Preston	The minimum Reynolds number for a turbulent boundary layer and the selection of a transition device. J. Fluid Mech., Vol.3, Part 4, p.373. January, 1958.

FIG. 1

Source of data :-

□ Clauser I¹⁵
△, ○ Bradshaw¹²



Equilibrium boundary layers

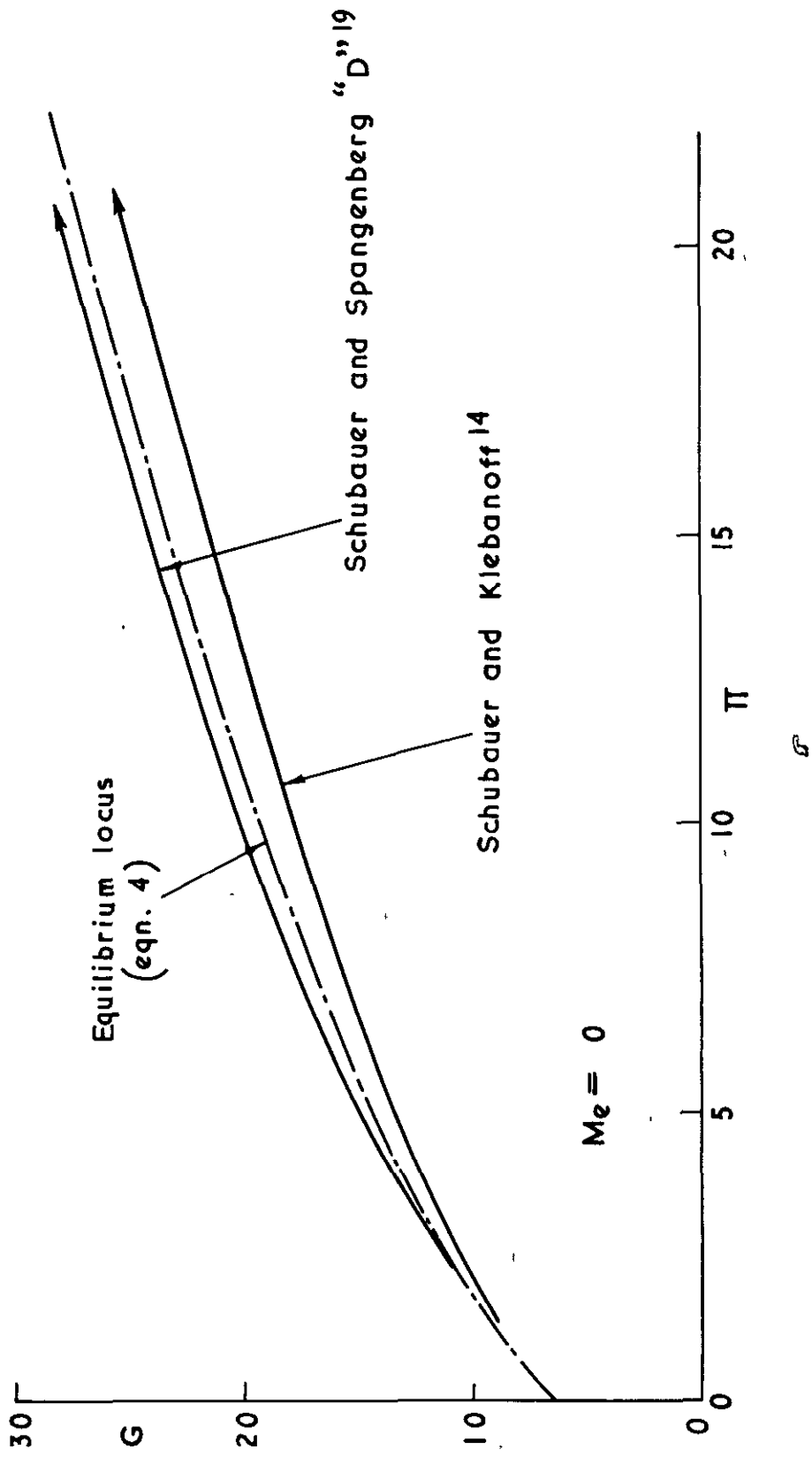
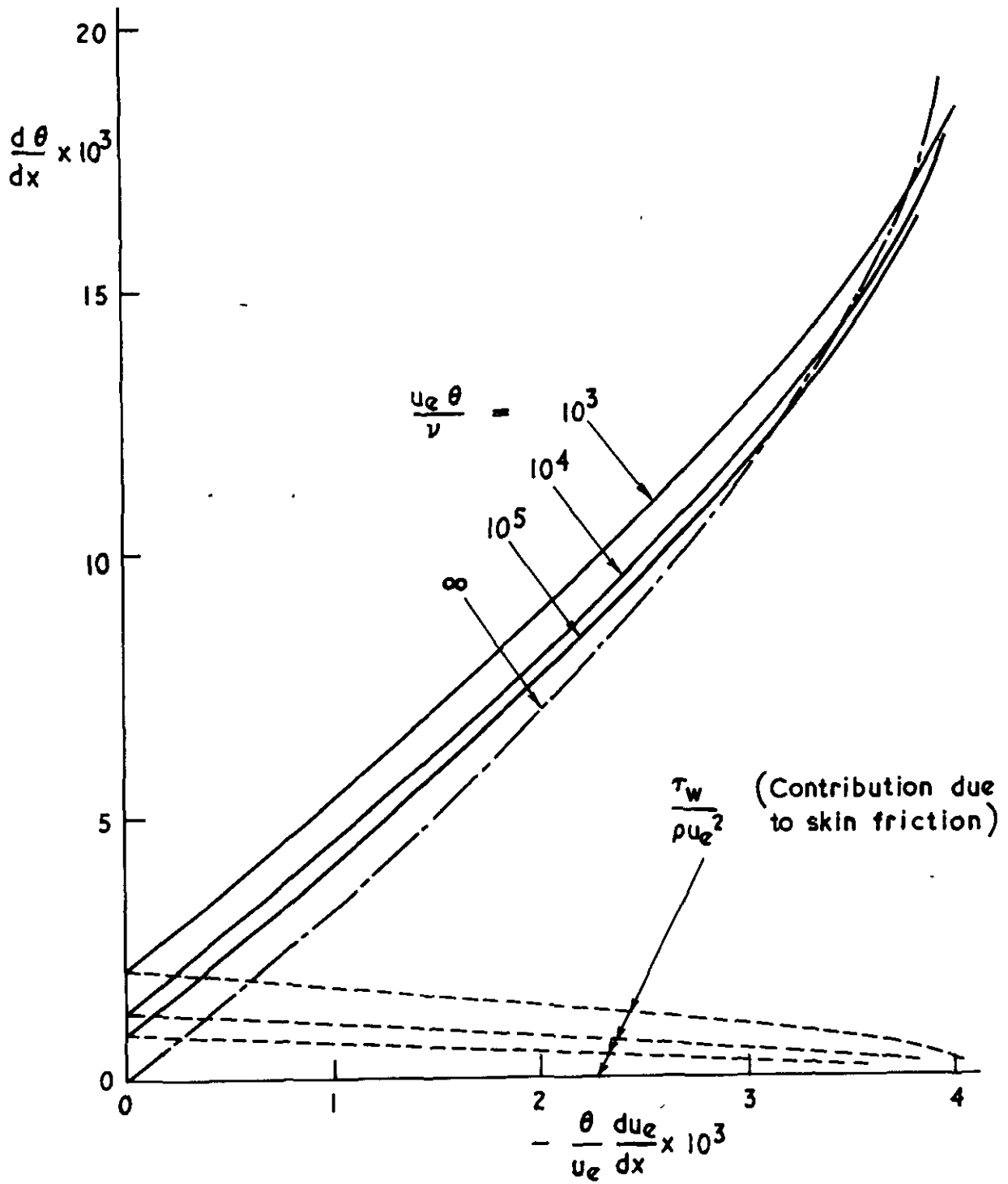


FIG. 2

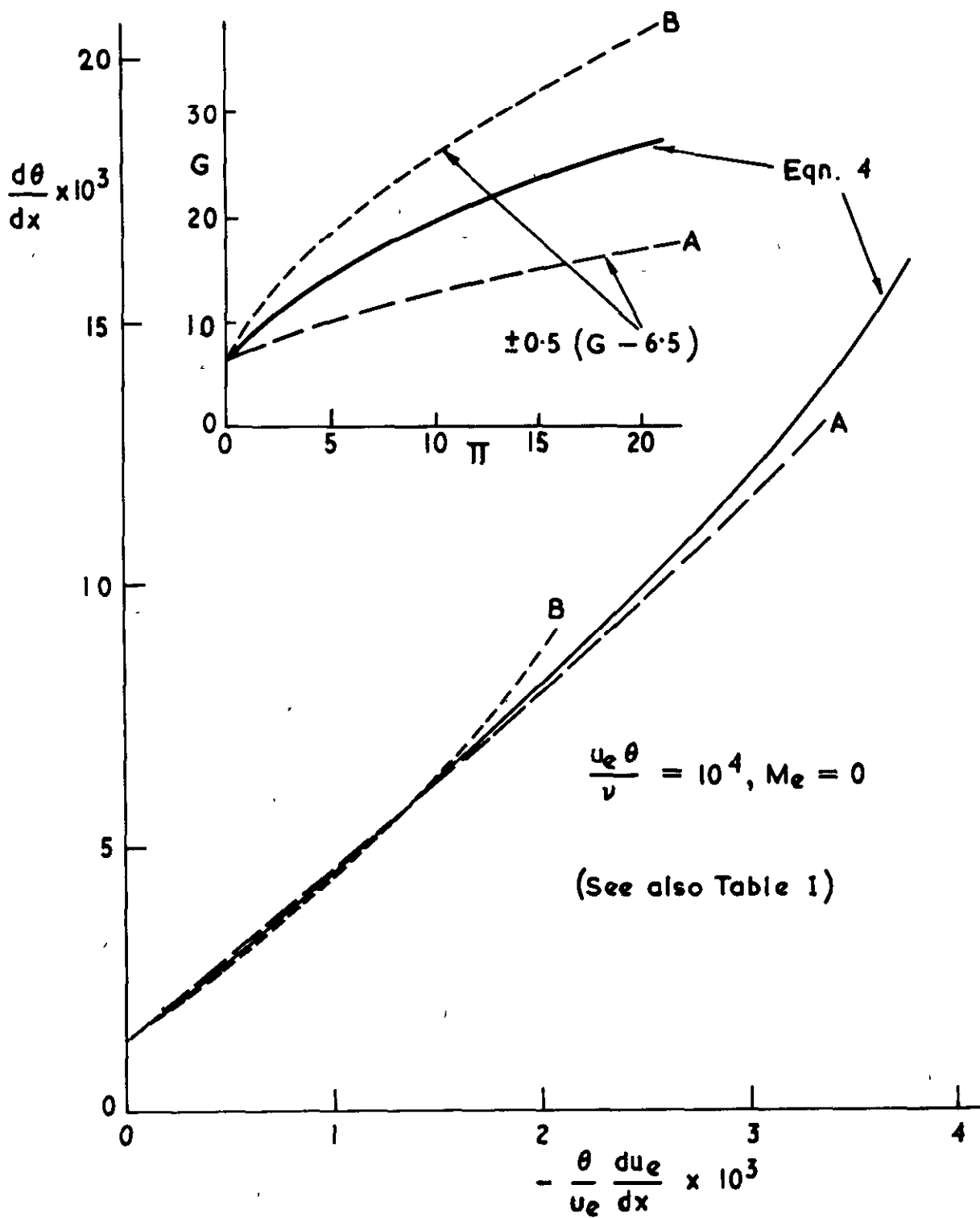
Proximity to local equilibrium — boundary layers with $\frac{d\pi}{dx} > 0$

FIG. 3



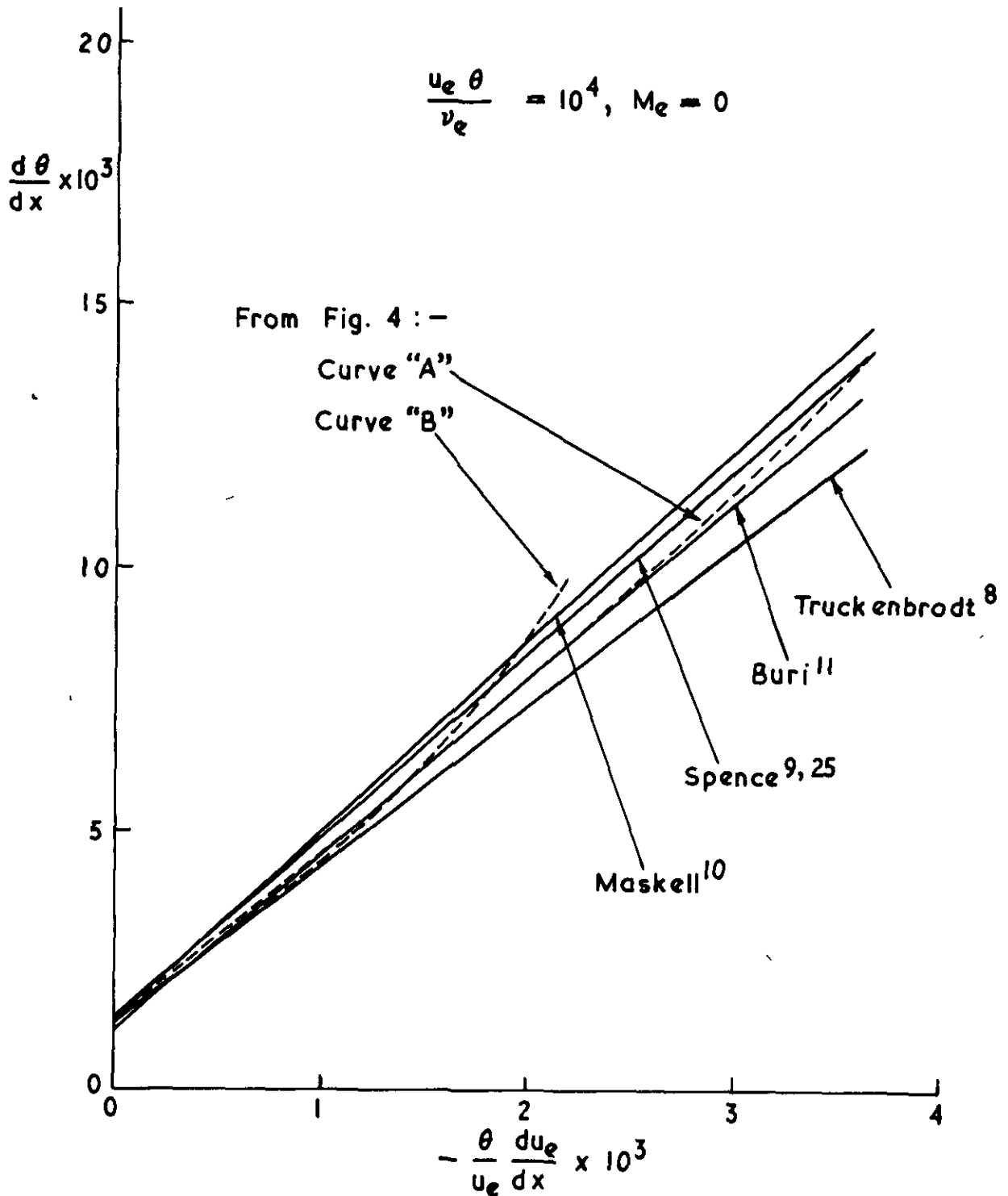
The momentum equation, using the local-equilibrium assumption ($M_e = 0$)

FIG. 4



Insensitivity of $d\theta/dx$ to departures from equilibrium

FIG. 5



Comparison with "quadrature methods"

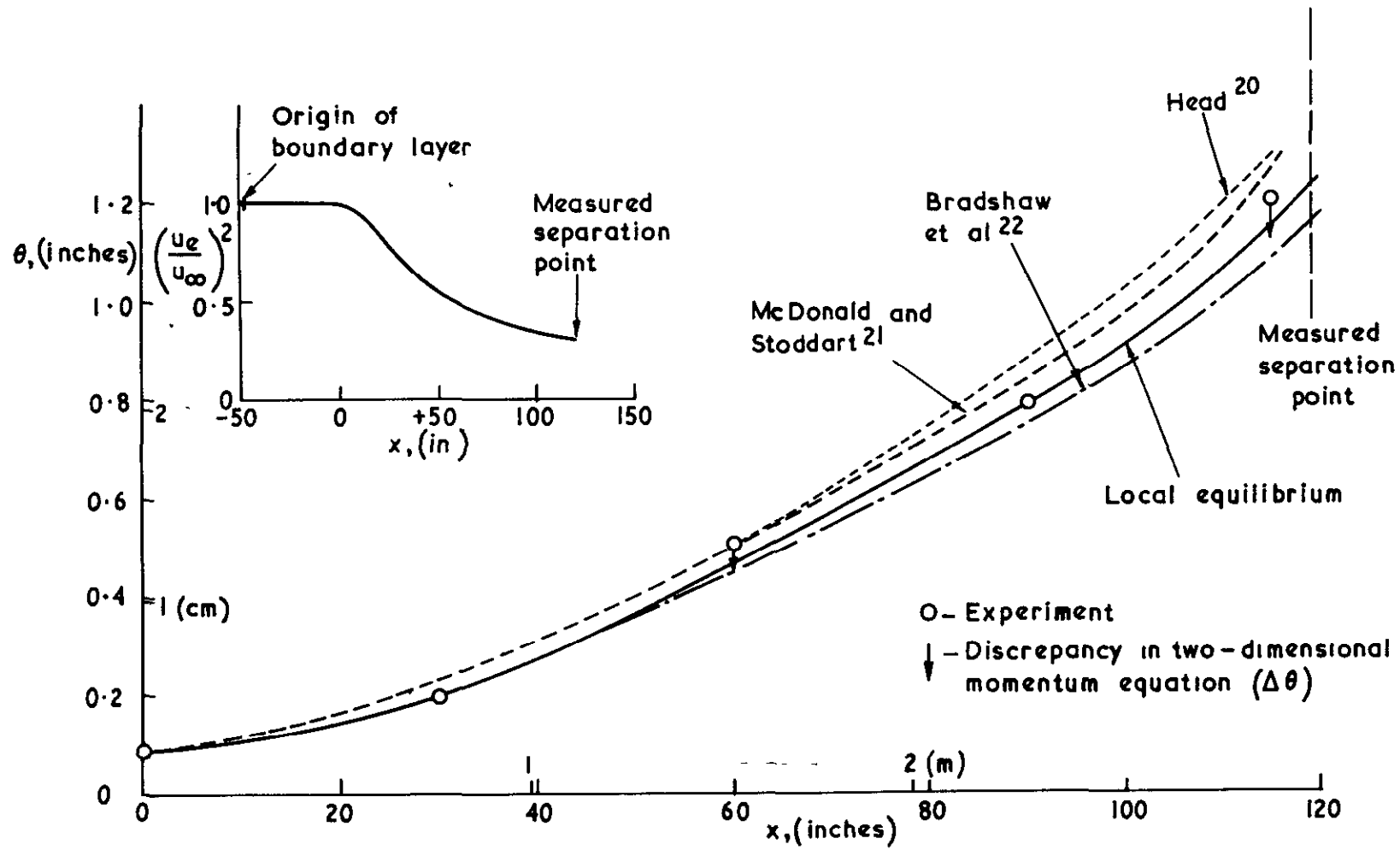
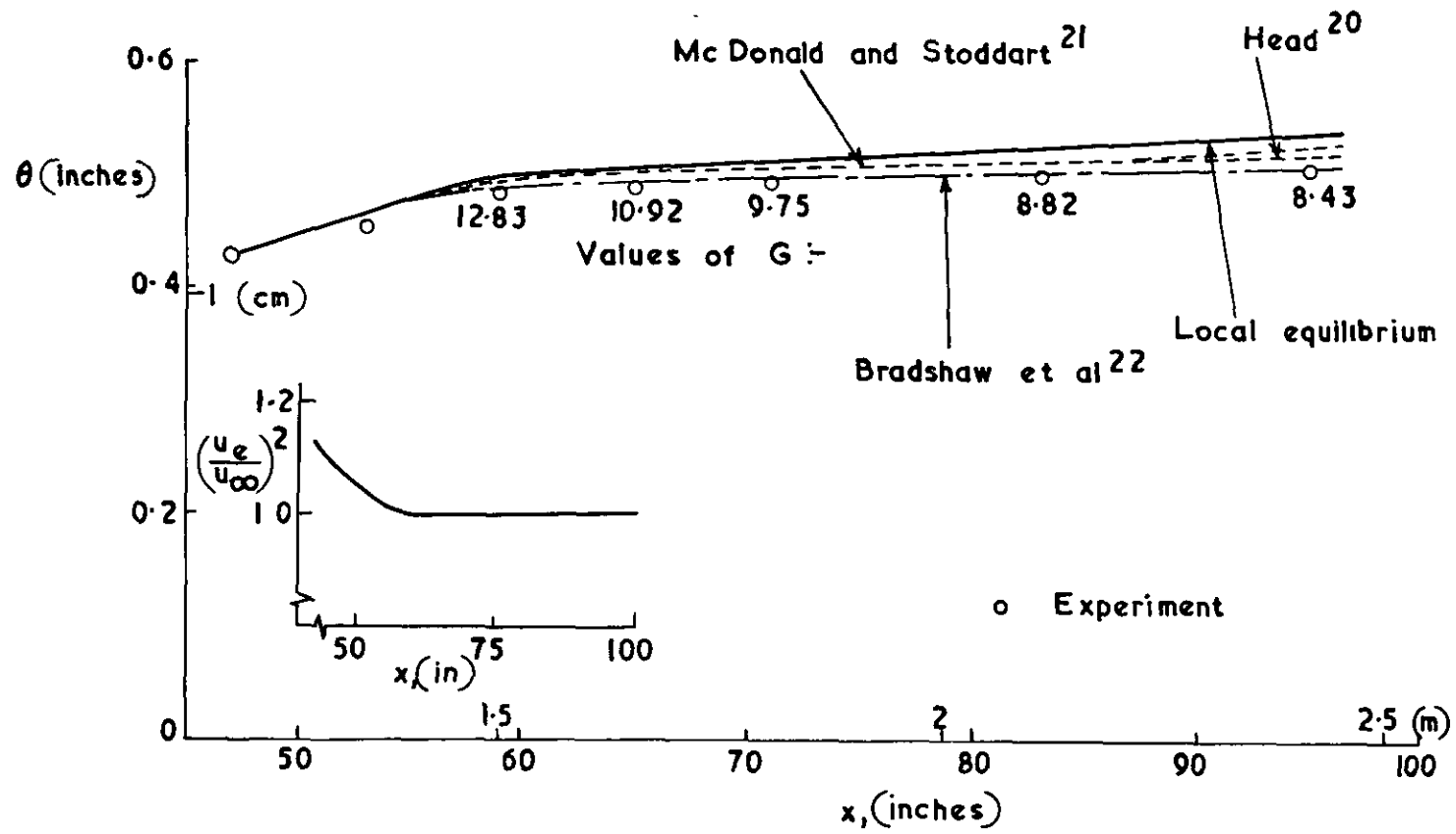


FIG. 6

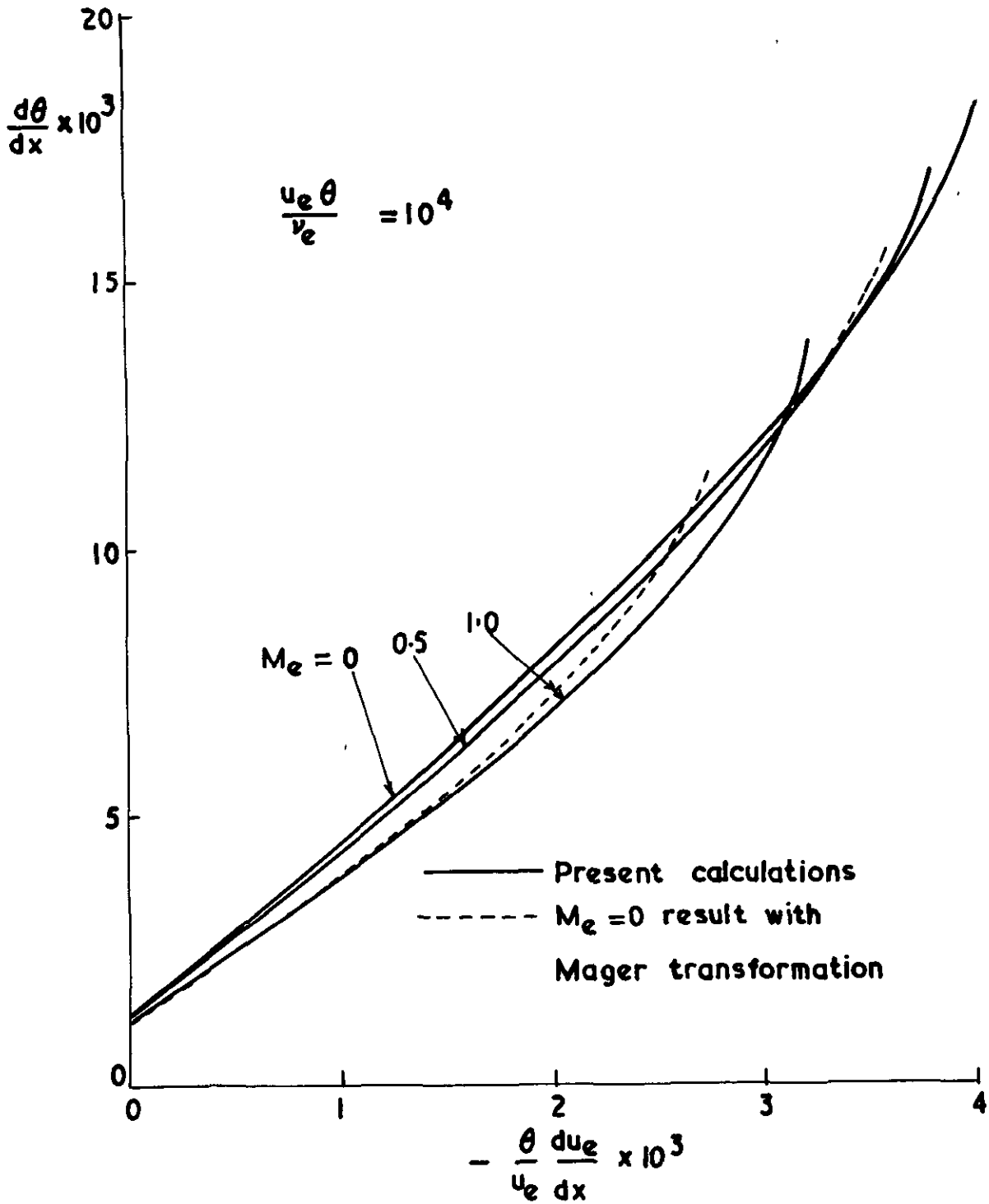
Comparison with experiment — Schubauer and Spangenberg "D"19



Comparison with experiment — Bradshaw and Ferriss 18

FIG 7

FIG. 8



The momentum equation, using the local - equilibrium concept

— compressible flow

D 89638/1/129528 K4 8/87 XL

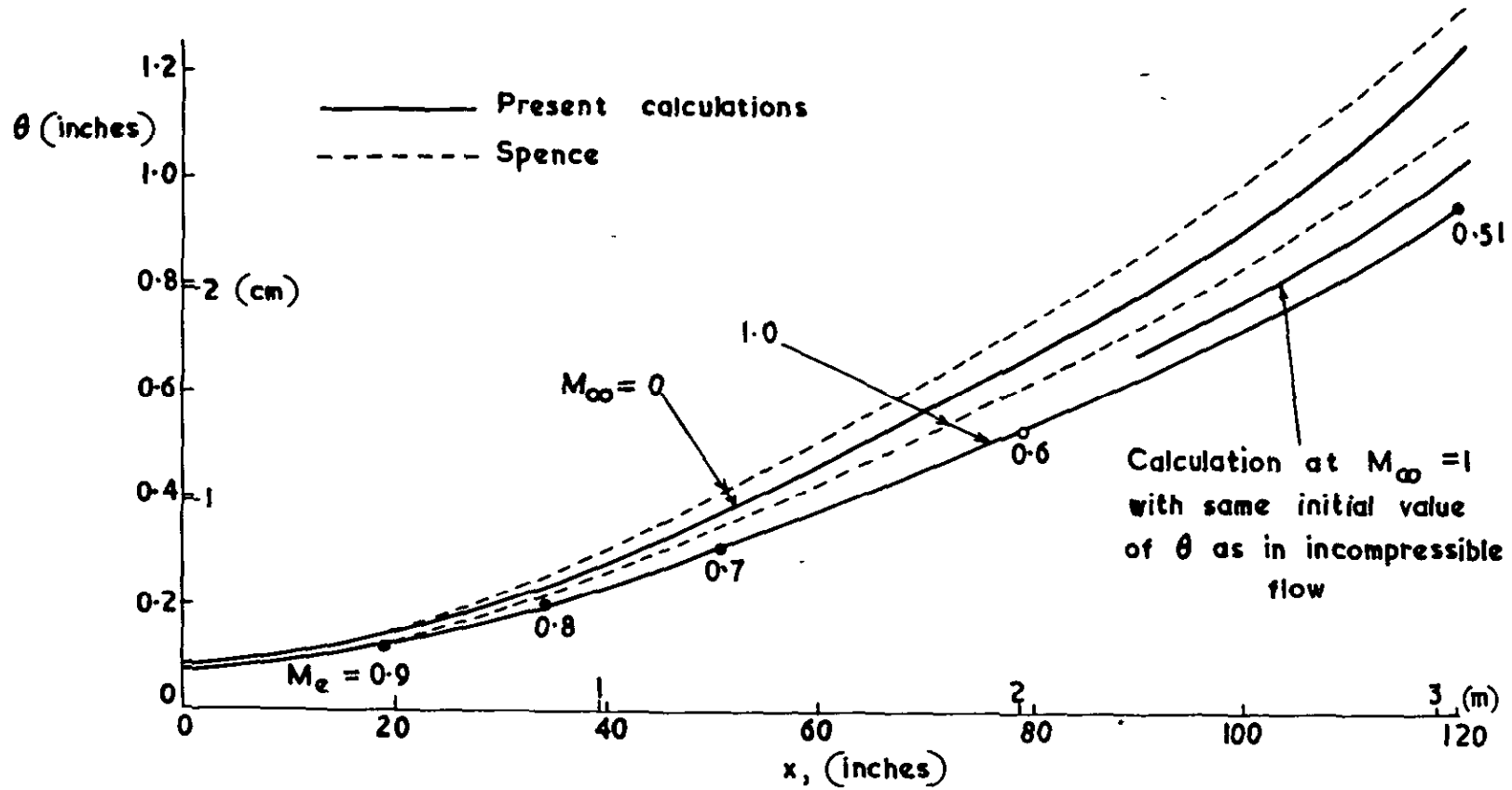


FIG. 9

Calculations in compressible flow, using same velocity distribution as in Fig 6.

A.R.C. C.P. No. 963

July, 1966.

Nash, J. F. and Macdonald, A. G. J.

THE CALCULATION OF MOMENTUM THICKNESS IN A TURBULENT
BOUNDARY LAYER AT MACH NUMBERS UP TO UNITY

For boundary layers of a class which includes those developing in "rooftop" pressure distributions, the small departures from local equilibrium which occur are shown to have an even smaller effect on the growth of momentum thickness. The assumption of precise local equilibrium thus provides a simple but accurate basis for predictions of momentum thickness, and a calculation method is formulated accordingly.

A.R.C. C.P. No. 963

July, 1966.

Nash, J. F. and Macdonald, A. G. J.

THE CALCULATION OF MOMENTUM THICKNESS IN A TURBULENT
BOUNDARY LAYER AT MACH NUMBERS UP TO UNITY

For boundary layers of a class which includes those developing in "rooftop" pressure distributions, the small departures from local equilibrium which occur are shown to have an even smaller effect on the growth of momentum thickness. The assumption of precise local equilibrium thus provides a simple but accurate basis for predictions of momentum thickness, and a calculation method is formulated accordingly.

A.R.C. C.P. No. 963

July, 1966.

Nash, J. F. and Macdonald, A. G. J.

THE CALCULATION OF MOMENTUM THICKNESS IN A TURBULENT
BOUNDARY LAYER AT MACH NUMBERS UP TO UNITY

For boundary layers of a class which includes those developing in "rooftop" pressure distributions, the small departures from local equilibrium which occur are shown to have an even smaller effect on the growth of momentum thickness. The assumption of precise local equilibrium thus provides a simple but accurate basis for predictions of momentum thickness, and a calculation method is formulated accordingly.

DETACHABLE ABSTRACT CARDS

© *Crown copyright 1967*

Printed and published by
HER MAJESTY'S STATIONERY OFFICE

To be purchased from
49 High Holborn, London W C.1
423 Oxford Street, London W 1
13A Castle Street, Edinburgh 2
109 St Mary Street, Cardiff
Brazennose Street, Manchester 2
50 Fairfax Street, Bristol 1
35 Smallbrook, Ringway, Birmingham 5
7 - 11 Linenhall Street, Belfast 2
or through any bookseller

Printed in England